

Practical 3D inversion of large airborne time domain electromagnetic data sets

1st **Dikun Yang**

University of British Columbia
6339 Stores Rd, Vancouver, Canada, V6T 1Z4
yangdikun@gmail.com

2nd **Douglas W. Oldenburg**

University of British Columbia
6339 Stores Rd, Vancouver, Canada, V6T 1Z4
doug@eos.ubc.ca

SUMMARY

In this paper we show that 3D inversion of large airborne time domain EM data, which is traditionally considered impractical, can be rapidly carried out by using a thoughtful workflow. In our 3D inversion algorithm, the number of cells in the mesh and the number of soundings are two factors that slow down the inversion. Therefore, we develop a strategy of adaptive mesh and sounding refinement to minimize the number of cells and the number of soundings required by the inversion. At the beginning, a coarse mesh and a few soundings are used to quickly build up a large-scale model. Then the mesh is refined and more soundings are added based upon their data misfit. At each iteration of the inversion, a certain number of soundings are randomly selected, and we change the data selection from iteration to iteration. This allows us to down-sample the field data without much loss of information. Once the large-scale model is obtained, we carry out some tile inversions that focus on smaller areas with a locally refined mesh to better resolve the small-scale features. The workflow is demonstrated by a synthetic example with 2121 transmitters that takes about 10 hours to be solved compared to about 150 hours if we had started the inversion on a fine mesh and used all of the transmitters. The methodology of speeding up the inversion by adaptive mesh and data refinement can also be applied to other EM surveys.

Key words: airborne, time domain, electromagnetic, three dimension, inversion

INTRODUCTION

In previous studies it has been shown that three-dimensional inversion of airborne time-domain electromagnetic (ATEM) data has the capability to resolve complex conductivity structure compared to traditional 1D inversion. However, there remain obstacles that slow down the application of 3D ATEM inversion for large datasets. Because an ATEM survey usually covers a large area and measures time-decaying signal at thousands or tens of thousands of locations, the number of model parameters and the number of transmitters (soundings) to be modelled can be prohibitively large for rigorous 3D inversion. Cox, et al. (2010) and Wilson, et al. (2010) address this type of problem by using an integral equation method with a footprint-based sensitivity reduction. Within the framework of the finite volume method, we propose a different way of inverting large ATEM datasets in

3D and show how to speed up the process by a thoughtful work flow that minimizes the number of model parameters and the number of transmitters used in an inversion. Additionally, this work flow also helps find the resolution limit of the data. Our work flow is showcased by a synthetic example.

The work flow is based on two principles: (1) ATEM data are redundant so not all the soundings need to be included in the inversion; (2) a 3D inversion can be carried out in a multi-scale manner so a finely discretised mesh (with a large number of model parameters) is not necessary until the large-scale features have been recovered. In order to minimize the number of model parameters and the number of transmitters, we develop a strategy that starts with a small number of transmitters and a very coarse mesh, and then adaptively refine the mesh and increase the number of transmitters. The soundings are selected randomly for each iteration of inversion; this allows under-sampling without bias. If the survey area is too large to be carried out in a single run at global scale, the entire area will be decomposed into smaller tiles and solved separately. As this procedure is driven by the data, it will stop if there is no need to refine the mesh and/or add more transmitters at the limit of data resolution.

Our synthetic example shows that this work flow can reconstruct a model that fits all of the observations from a few thousand transmitters reasonably well in a few hours on a desktop computer or a single node of an average cluster. This makes our algorithm practical for daily exploration problems.

INVERSION ALGORITHM

The forward modelling and inversion algorithms used in this research are described in Oldenburg, et al. (2008). Maxwell's equations are discretised by a 3D finite volume method in space and a backward Euler method in time. This results in a matrix equation of the forward modelling at each time step,

$$\mathbf{A}(\Delta t, \sigma) u = q, \quad (1)$$

where \mathbf{A} is a sparse symmetric coefficient matrix determined by the spatial discretization (mesh), the length of the time step Δt and the conductivity model σ ; u is the field to be solved (here we use H-field formulation); and q is the right-hand-side representing the boundary conditions and the sources. In order to solve the forward problem of multiple transmitters in an ATEM survey, we factorize the \mathbf{A} matrix into a Cholesky decomposition. Once the \mathbf{A} matrix is factorized and stored, many transmitters can be quickly solved, but if the length of time step and/or the conductivity model changes, the \mathbf{A} matrix must be re-factorized. Therefore, for a given conductivity model, the time required by a forward modelling depends

upon the mesh (the number of cells), the number of factorizations (the number of different Δt), the number of time steps and the number of transmitters. For the ATEM data, the number of factorizations and the number of time steps are primarily determined by the time channels of the system, so the bottlenecks are the fineness of the mesh and the large number of transmitters.

Our inversion is based on a Gauss-Newton method (Oldenburg, et al., 2008), in which a model update Δm is sought by solving

$$(\mathbf{J}^T \mathbf{J} + \beta \mathbf{W}^T \mathbf{W}) \Delta m = -g, \quad (2)$$

where \mathbf{J} is the sensitivity matrix, \mathbf{W} is a sparse regularization matrix, β is the trade-off parameter and g is the gradient of the objective functional. The sensitivity \mathbf{J} is kept in a factored form so that it, or its transpose, can be applied to a vector. This is all that is required since the system (2) is solved with a pre-conditioned conjugate gradient (CG) solver. Each \mathbf{J} -vector or \mathbf{J}^T -vector multiplication is equivalent to a complete forward modelling in Equation (1). Supposing that a typical Gauss-Newton inversion requires 5 β -iterations, and the maximum number of CG iterations is 10, then the total number of forward modellings to complete in an inversion is at least about 100. If the forward modelling is not fast enough, the inversion will be too slow to be practical.

ADAPTIVE MESH AND SOUNDING REFINEMENT (AMSR)

Since it is the number of cells in a mesh and the number of soundings (transmitters/sources) that are bottlenecks for a fast inversion, we design the workflow to be carried out in a multi-scale manner: a coarse mesh and few soundings at the beginning; then refinement of the mesh and/or adding more soundings when necessary. There are several terms used in the work flow:

(1) Random sounding selection. Randomly select some soundings out of the total N ATEM soundings based on uniform distribution. A good random selection is the one that does not have significant clustering of the soundings.

(2) Global data misfit. Φ_d^G is a global data misfit for all soundings in the survey area. Usually this is estimated by randomly selecting N_g soundings where $N_g \leq N$, carrying out the forward modelling at these stations and evaluating the misfit. This number is normalized by N_g , so a value near unity means an acceptable fit.

(3) Proposed (model) update. This is the model update sought by inverting the N_g soundings for one Gauss-Newton iteration. A proposed update can be justified by a post-iteration estimated data misfit that is (sufficiently) smaller than the pre-iteration misfit.

(4) Mesh refinement. Switch the working mesh from coarse to fine. During this transition, the old model on the coarse mesh is also passed over to have a new representation on the fine mesh. The number of cells will increase dramatically after the refinement, which means enhanced resolving power but much more computational cost.

The basic idea of AMSR is to keep the mesh as coarse as possible and to keep the number of soundings as few as possible, while ensuring a sufficient decrease of the estimated data misfit. The AMSR always tries to propose a model update with the current mesh and current number of soundings. If the proposed update is not justified, one

possible reason is that the number of soundings is not large enough so that the inversion is misled by too few soundings. Then AMSR will increase the number of soundings, reselect a new group of random soundings, run another iteration and check if more soundings provide a valid update. Sometimes increasing the number of soundings cannot help the reduction of the data misfit. This signals the need for a finer mesh, on which small-scale features can be resolved and data from earlier time channels can be better fit. This procedure is repeated until the target data misfit or the resolution limit of data is achieved. The AMSR is summarized as a flowchart in Figure 1.

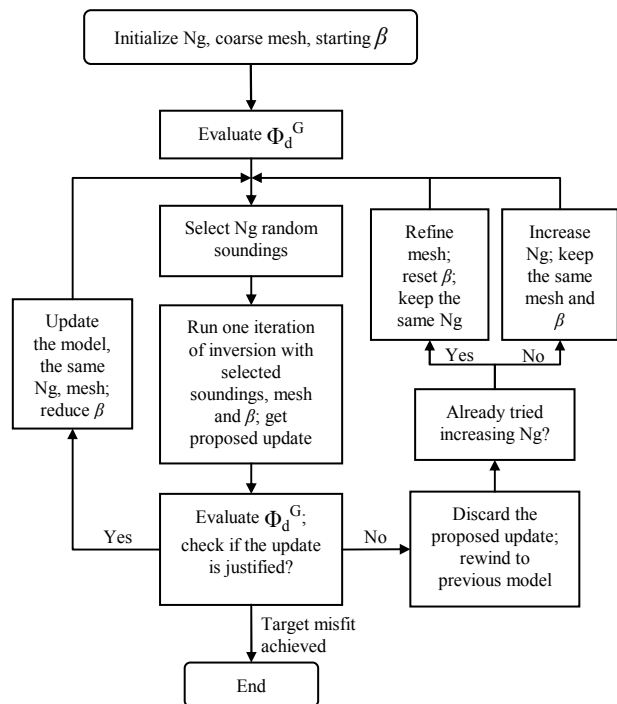


Figure 1. Flowchart of adaptive mesh and sounding refinement (AMSR). N_g is the number of soundings used in the global inversion from the entire survey; β is the trade-off parameter in Equation (2). If the mesh is refined, β needs to be re-evaluated and reset.

TILE INVERSION OF LARGE SURVEY

For a large ATEM survey, it is necessary to subdivide the entire survey area into tiles and invert these tiles separately after the large-scale structure has been built up from a coarse mesh inversion. There are two reasons for tiling. The first pertains to computational difficulties. As the mesh gets refined, the problem may become too large to be handled. The second pertains to complexity of the conductivity model. Some parts of the survey area may require inversion with more soundings and/or finer meshes.

The inversion strategy for the tilings is similar to that outlined for the global inversion on the coarse mesh. We need to introduce two additional items:

(1) Tile data misfits. Φ_d^T is data misfit for all N_T soundings in the survey area concerned with the tile of interest. Usually this is estimated by randomly selecting N_t soundings where $N_t \leq N_T$, carrying out the forward modelling at these stations and evaluating the misfit. This number is

normalized by N_t , so a value near unity means an acceptable fit.

(2) Mixed mesh. This is used for a tile inversion. Fine cells are used within the tile of interest while a mixture of coarse and fine cells are defined on the remainder of the volume.

The starting model of each tile inversion is derived from the global inversion of the entire survey on coarse mesh. This model is transferred to a mixed mesh and the inversion carried out as per the flow chart (except that Φ_d^T replaces Φ_d^G). Once the tile inversions are completed they are stitched together to generate the final model for interpretation. The AMSR and the tile inversion are demonstrated with the use of a synthetic example in the following section.

SYNTHETIC EXAMPLE

In this example, an ATEM survey is carried out over a 2×2 km area with flat topography. The towed transmitter and receiver fly at a constant height 50m above the surface. The transmitter loop is a 10×10 m square loop and the receiver sits at the centre of the transmitter. The transmitter current waveform is a step-off and 21 time channels from 0.1~10ms are recorded. The synthetic model comprises both large-scale features (0.01S/m overburden, 0.05S/m eastern conductive basement and 0.02S/m south-western basement) and small-scale anomalies, which are many 0.1S/m buried blocks with variable geometries and random locations (Figure 2).

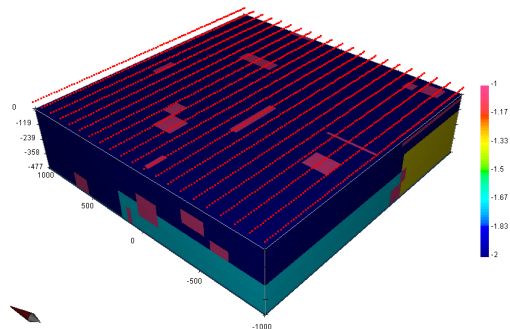


Figure 2. The conductivity model and sounding locations of our synthetic example. There are 21 lines with 100m line spacing; along each line there are 101 soundings with in-line sounding spacing 20m. The colour map is in log-scale. Sounding locations are indicated by the red dots.

Global Inversion

We start with a global inversion based on a uniform mesh over the entire area. The goal is to rapidly build up the large-scale conductivity model. Details of the global inversion are summarized in Table 1. The initial model of AMSR iteration 1 is 0.01S/m half-space. The starting mesh has the smallest cell size 200m, which is very coarse in this conductivity environment. Iteration 2 only slightly improves the data misfit, so 10 more soundings are added for iteration 3. In iteration 5, the proposed update is not justified, so 10 more soundings are added. However, adding soundings to iteration 6 does not help the data misfit; we need to refine the mesh for iteration 7. Φ_d^G is evaluated using $N_g = 100$ in the global inversion. Although the ending estimated data misfit is 1.89, a value greater than unity, we notice that those major contributors of the misfit are from early time channels at a few

locations and we should focus on local anomalies by carrying out tiled inversions.

AMSR iteration	N_g	Pre-iter. Φ_d^G	Post-iter. Φ_d^G	Cell size (m)	β	CPU time (m:s)	Notes
1	40	20.89	15.84	200	2.11	6:18	
2	40	15.84	15.34	200	0.42	8:34	
3	50	13.03	12.27	200	0.42	10:36	+ Ns
4	50	12.27	8.98	200	8.4E-2	11:21	
5	50	8.98	12.68	200	1.7E-2	11:15	
6	60	8.98	10.57	200	1.7E-2	13:01	+ Ns
7	60	7.31	4.75	100	4	17:24	refine
8	60	4.75	3.92	100	0.8	24:01	
9	60	3.92	2.36	100	0.16	23:24	
10	60	2.36	1.89	100	3.2E-2	23:12	

Table 1. Summary of the global inversion. Iterations 1 ~ 6 (before the mesh refinement) are carried out on an Intel i7 960 desktop computer. Iterations 7 ~ 10 are on a computer with 2 Intel Xeon X5660 CPUs. The total CPU time of the global inversion is about 2.5h.

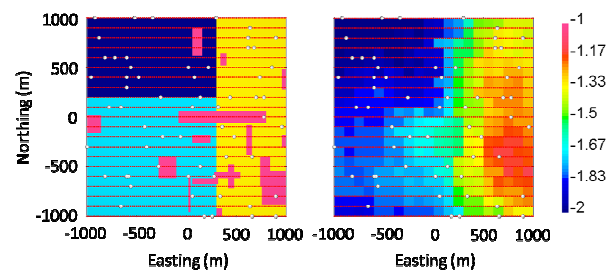


Figure 3. Depth slices of the true conductivity model (left) and the recovered conductivity model by the global inversion (right) at depth of 250m. Red dots are sounding locations of the entire survey. The 60 soundings used in the last iteration of the global inversion are highlighted by white dots.

One slice of the model obtained by the global inversion is compared with the true model in Figure 3. It is evident that the global inversion successfully revealed the large-scale structures. The soundings required by our workflow are only a small portion of the entire data set.

Tile Inversions

The entire survey area is subdivided into four tiles, which are referred as SW (southwest), SE (southeast), NW (northwest) and NE (northeast). The 100m-cell mesh from the global inversion is locally refined to 50m cell for each tile inversion (see example of the NW tile mesh in Figure 4). At the global scale we still select the same number of soundings as the global inversion, but add 40 more soundings within the tile. The soundings outside the tile stabilize the model update in the outer regions. This facilitates a seamless stitch of tile models at the end.

Within each tile, the AMSR is still applied. However, as the estimated data misfit gets close to unity, mesh refinement and adding more soundings are not necessary. Table 2 summarizes the four tile inversions. It is important to realize that the global inversion has fit the late time data well but does not adequately fit the early times. Before each tile inversion, the estimated data misfit of the first 5 time channels is always greater than that from all the time channels. This is especially true in the SE and NE tiles where the ground is more conductive and early time channels in these areas are not

properly modelled on the 100m-cell mesh. The misfit for the early time channels can be reduced only by having a finer mesh.

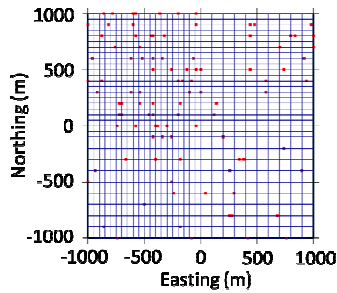


Figure 4. Locally refined mesh for the NW tile inversion. The cell size inside the NW tile is 50x50m, while the rest of the mesh still has 100x100m (or 50x100m) cells. Totally 100 soundings are inverted; 60 of them are randomly selected at the global scale and 40 of them are within the NW tile.

AMSR iteration	Nt	Pre-iter. Φ_d^T (all TC)	Pre-iter. Φ_d^T (TC 1~5)	Post-iter. Φ_d^T (all TC)	Post-iter. Φ_d^T (TC 1~5)	β	CPU time (m:s)
SW 1	60+40	0.74	1.23	0.55	1.07	2.34	81:39
SE 1	60+40	1.65	2.12	1.35	1.65	2.20	50:54
SE 2	60+40	1.35	1.65	0.44	0.79	0.44	70:28
NW 1	60+40	1.15	1.70	0.85	1.03	3.08	58:39
NE 1	60+40	1.55	4.59	1.12	2.97	2.80	64:04
NE 2	60+40	1.12	2.97	0.97	1.66	0.56	70:55
NE 3	60+40	0.97	1.66	0.42	0.84	0.11	70:06

Table 2. Summary of the global inversions. The estimated data misfits of the first 5 time channels are listed to show the tile inversions improve the data misfit of early time channels. Data misfits are all from the soundings in the tile. There is no increase of Nt and mesh refinement during each tile inversion. The total CPU time of the tile inversions is about 7.8h on a computer with 2 Intel Xeon X5660 CPUs.

After each tile inversion has reduced the data misfit for the first 5 time channels below, or close to, unity, the four tiles are stitched together to form a final model for interpretation (Figure 5). The recovered final model has correct information about the basement and also presents some small-

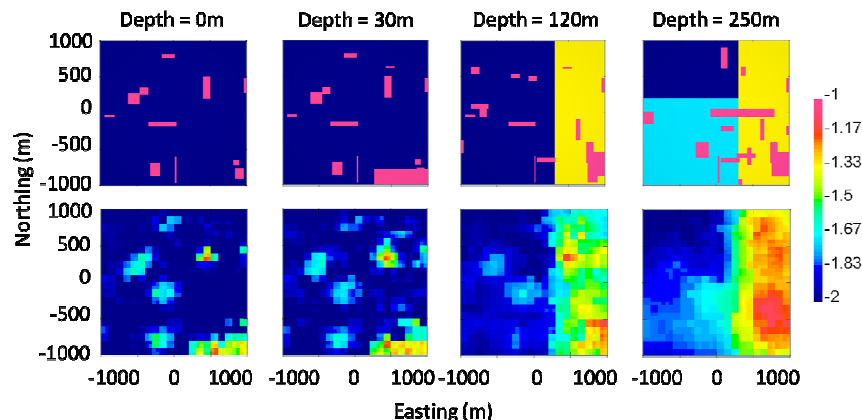


Figure 5. Depth slices of the true conductivity model (top row) and the conductivity model recovered by our inversion workflow (bottom row). The inversion successfully revealed the conductivity contrast of the basement and located some conductors that are near surface or clustered.

scale anomalies near surface that have good correspondence with the true model. Because of the limitation of EM diffusion, some isolated small conductors at depth are not seen in the inversion model. We also ran a benchmark forward modelling on the 50m-cell mesh with all of the 2121 soundings, which takes 90 minutes on one node of the cluster. If the 2121 transmitters had been run from the outset on the final 50m-cell mesh, the full inversion would have required about 150 hours and significantly more memory requirements.

CONCLUSIONS

In this paper we have developed a workflow methodology that allows efficient 3D inversion of large ATEM data sets. A synthetic example has demonstrated the validity of our workflow. There are two important conclusions we can draw from our example:

(1) A fine mesh is not necessary at the early stage in an inversion. By using a coarse mesh, the large-scale model can be rapidly built up. A multi-scale method is thus appropriate.

(2) ATEM data are redundant and there is no necessity to use all of the soundings in an inversion at one time. Random selection of soundings and changing soundings from iteration to iteration allow us to down-sample the soundings without much loss of information.

ACKNOWLEDGMENTS

The authors thank the members of the MITEM Consortium and NSERC for their financial support.

REFERENCES

- Cox, L. H., G. A. Wilson, and M. S. Zhdanov, 2010, 3D inversion of airborne electromagnetic data using a moving footprint: *Exploration Geophysics*, 41, 250-259.
- Oldenburg, D. W., E. Haber, and R. Shekhtman, 2008, Forward modelling and inversion of multi-source TEM data: *SEG Technical Program Expanded Abstracts*, 27, 559-563.
- Wilson, G. A., L. H. Cox, and M. S. Zhdanov, 2010, Practical 3D inversion of entire airborne electromagnetic surveys: *Preview*, 2010, 29-33.